

## Hydrothermal synthesis of cobalt oxide nanoparticles: Its optical and magnetic properties

M. Yarestani<sup>1</sup>, A.D. Khalaji<sup>2\*</sup>, A. Rohani<sup>3</sup>, D. Das<sup>4</sup>

<sup>1</sup>Department of Chemical Engineering, College of Engineering, Shahrood Branch, Islamic Azad University, Shahrood, Islamic Republic of Iran

<sup>2</sup>Department of Chemistry, Faculty of Science, Golestan University, Gorgan, Islamic Republic of Iran

<sup>3</sup>Research institute of Petroleum Industry, the west entrance to Azadi stadium, Olympic Blv., Tehran, Islamic Republic of Iran

<sup>4</sup>Department of Chemistry, The University of Burdwan, Burdwan, West Bengal, India

Received: 21 April 2014 / Revised: 28 May 2014 / Accepted: 5 July 2014

### Abstract

Cobalt oxide (Co<sub>3</sub>O<sub>4</sub>) nanoparticles have been synthesized by hydrothermal method using mixture of cobalt(II)chloride, Triton X-100 and KOH in an autoclave at 180 °C for 6 h followed by heating at 400 °C for 3 h in air. The product have been characterized by Fourier transform infrared (FT-IR), UV-Vis spectroscopy, powder X-ray diffraction (XRD), scanning electron microscopy (SEM) and transmission electron microscopy (TEM). Optical properties of the Co<sub>3</sub>O<sub>4</sub> nanoparticles have revealed the presence of two band gaps, viz. 2.9 and 2.4 eV. Data from vibrating sample magnetometer (VSM) confirm the purity of the product along with single phase paramagnetic behavior.

**Keywords:** Cobalt oxide; XRD; SEM; TEM; Optical properties.

### Introduction

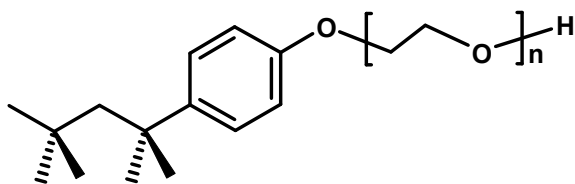
Cobalt oxide (Co<sub>3</sub>O<sub>4</sub>) nanoparticles exhibit interesting properties and applications when compared with their bulk, such as lithium storage [1], gas sensing [2] and electro-catalyst [3]. The most stable phase of cobalt oxides (Co<sub>3</sub>O<sub>4</sub>) with a direct band gap of 1.48-2.19 eV, is used as an *n*-type semiconductor and received considerable attention [1-5]. Various methods have been developed to synthesize Co<sub>3</sub>O<sub>4</sub> nanoparticles, including the hydrothermal [4,5], microwave-assisted [6] and reverse micelles [7]. However, hydrothermal method is green and less expensive. Synthesis of Co<sub>3</sub>O<sub>4</sub> nanoparticles via hydrothermal method generally requires reducing and precipitating agents. Until now, various nanoparticles of Co<sub>3</sub>O<sub>4</sub> have been prepared by different methods [8-12]. Therefore, development of facile and rapid method to prepare high purity Co<sub>3</sub>O<sub>4</sub>

nanoparticles having various morphologies [1-14] is highly desirable. Recently, our group has been synthesized metal oxides nanoparticles via thermal decomposition method of transition metal Schiff base complexes [15,16]. Herein, we report synthesis, characterization and possible growth mechanism of Co<sub>3</sub>O<sub>4</sub> nanoparticles by hydrothermal method.

### Materials and Methods

All reagents and solvents for synthesis and analysis were commercially available and used as received without further purifications. X-ray powder diffraction (XRD) pattern of the complex was recorded on a Bruker AXS diffractometer D8 ADVANCE with Cu-K $\alpha$  radiation with nickel beta filter in the range  $2\theta = 4^\circ - 84^\circ$ . Fourier Transform Infrared spectra were recorded as a KBr disk on a FT-IR Perkin-Elmer spectrophotometer.

\* Corresponding author: Tel: +98 171 2245882; Fax: +98 171 2245964; Email: alidkhalaji@yahoo.com



Scheme 1. Chemical structure of Triton X-100

The scanning electron microscopy (SEM) images were obtained from a Philips XL-30ESEM. The transmission electron microscopy (TEM) images were obtained from a JEOL JEM 1400 transmission electron microscope with an accelerating voltage of 120 kV. Optical absorption spectra are recorded at room temperature on a Cary 100 UV-visible spectrophotometer (VARIAN EL 12092335) having wavelength range of 200 – 700 nm. A homogeneous suspension in distilled water, obtained through sonication (for 10 minutes) of well dispersed sample is used for UV-vis studies. Magnetic measurements are made at room temperature using a vibrating sample magnetometer (VSM) (BHV-55, Riken, Japan).

#### Preparation of $Co_3O_4$ nanoparticles

Cobalt chloride (2.5 mmol) is dissolved in 40 mL distilled water and a certain amount of surfactant (1%, w/w, Triton X-100, Scheme 1) is added subsequently. Aqueous KOH and surfactant solutions are added drop wise until dark green solution is obtained. The resultant mixture is transferred into a 100 mL sealed teflon-lined autoclave and kept at 180 °C for 6 h. After cooling the autoclave to room temperature, the dark precipitate is obtained, filtered, washed with distilled water followed by absolute ethanol, and dried at 90 °C for 6 h under vacuum. Thus obtained  $Co_3O_4$  compound is labeled as MY-1. MY-1 is further heated at 400 °C for 3 h in presence of air and the product is labeled as MY-2.

## Results and Discussion

Triton X-100, used as stabilizing agent in nanocolloidal system is absorbed on the surface of cobalt ion.  $H_2O_2$  and KOH function as homogeneous precipitating agents. The probable chemical reactions are as follows:

- $CoCl_2 + 2 KOH \rightarrow Co(OH)_2 \downarrow + 2 KCl$
- $3 Co(OH)_2 \downarrow + H_2O_2 \rightarrow Co_3O_4 \downarrow + H_2O$

#### FTIR spectra

Figure 1a and 1b show FTIR spectra of  $Co_3O_4$  nanoparticles (MY-1 and MY-2). The strong bands at 576 and 670  $cm^{-1}$  for MY-1 and 662 and 568  $cm^{-1}$  for MY-2, belonging to the spinel structure of  $Co_3O_4$  [5]. The former peak at about 660-670  $cm^{-1}$  is attributed to the stretching vibration mode of Co-O in which Co is  $Co^{+2}$  and is tetrahedrally coordinated. The latter one at 568-576  $cm^{-1}$  can be assigned to Co-O of octahedrally coordinated  $Co^{+3}$ . The two bands appeared at 3551 and 1610  $cm^{-1}$  have been assigned to the stretching and bending vibrations of adsorbed water molecule on  $Co_3O_4$  nanoparticles [4].

#### PXRD studies

The as-prepared  $Co_3O_4$  nanoparticles have been characterized by X-ray powder diffraction (XRD) (Fig. 2). The XRD patterns of MY-1 and MY-2 are slightly different, because MY-2 is a mixed  $Co_3O_4$  and CoO phases. All diffraction peaks at  $2\theta = 19$  (111), 31 (220), 37 (311), 39 (222), 45 (400), 56 (422), 59 (511) and 66 (440) displayed on the PXRD pattern of MY-1 and MY-2 can be indexed to the cubic  $Co_3O_4$  structure (JCPDS No. 43-1003). No characteristic peaks of other impure phases like CoO ( $2\theta = 20$  (111), 23 (220), 37 (220) and 38 (311)) in the XRD of MY-1 could be detected, indicating that the  $Co_3O_4$  products were of high purity. The average size of the  $Co_3O_4$  nanoparticles have been determined using the Debye-Scherrer formula ( $D = 0.9 \lambda / \beta \cos \theta$ ), found as 26.6 nm for MY-1 and 21.3 nm for MY-2.

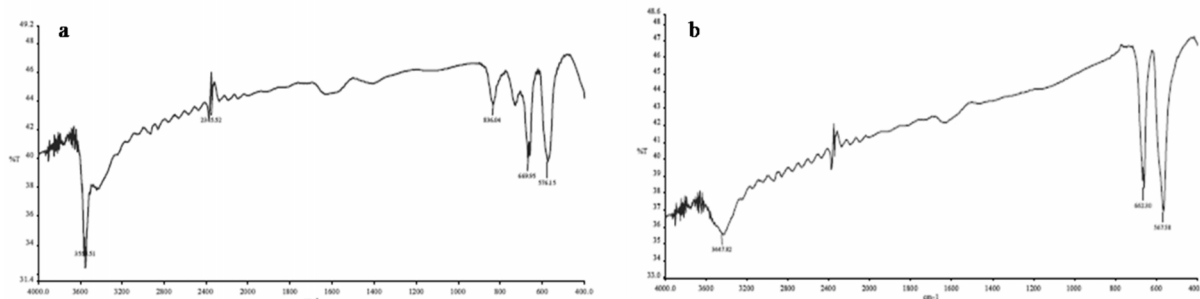


Figure 1. FTIR spectra of  $Co_3O_4$  nanoparticles MY-1 (a) and MY-2 (b).

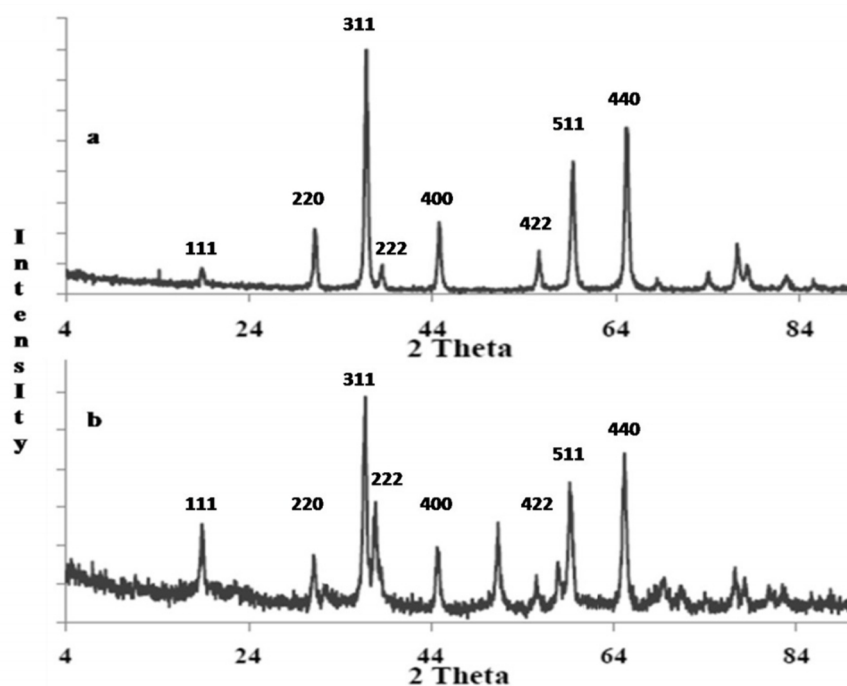


Figure 2. PXRD patterns of  $\text{Co}_3\text{O}_4$  nanoparticles: MY-1 (a) and MY-2 (b).

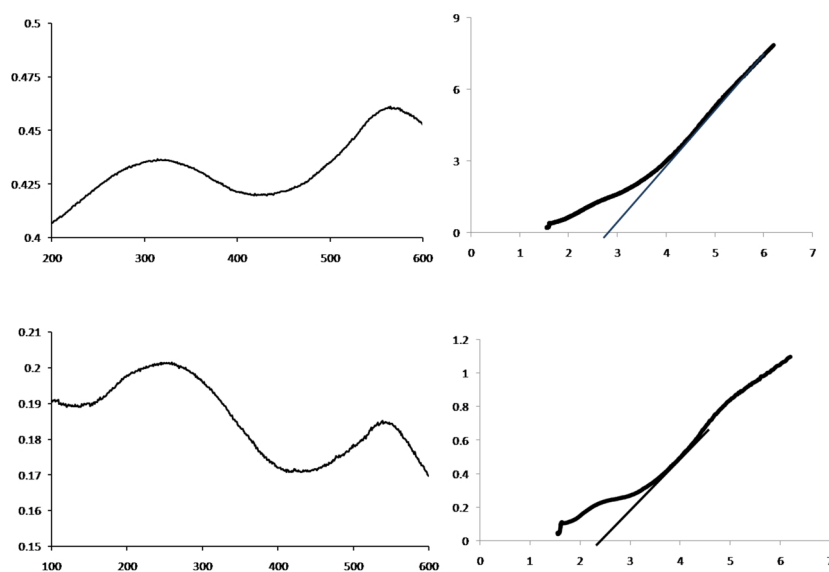


Figure 3. The UV-Vis and band gap of  $\text{Co}_3\text{O}_4$  nanoparticles: MY-1 (top) and MY-2 (bottom).

#### Optical and VSM studies

The optical absorption spectra of the  $\text{Co}_3\text{O}_4$  nanoparticles have been carried out using UV-vis spectroscopy. The optical absorption profile (Fig. 3) shows two bands at 560 and 315 nm for MY-1 and 550 and 250 nm for MY-2, which indicating ligand-metal charge transfer events  $\text{O}^{2-} \rightarrow \text{Co}^{3+}$  and  $\text{O}^{2-} \rightarrow \text{Co}^{2+}$ , respectively and are expected for  $\text{Co}_3\text{O}_4$  [12]. The direct band gaps energy of the  $\text{Co}_3\text{O}_4$  nanoparticles are 2.9 eV for MY-1 and 2.4 eV for MY-2 [17].

The magnetic behavior of the  $\text{Co}_3\text{O}_4$  nanoparticles has been investigated at room temperature. The fine hysteresis loop in Fig. 4 is characteristics of paramagnetic behavior, although bulk  $\text{Co}_3\text{O}_4$  shows anti-ferromagnetic behavior.

#### SEM and TEM images

SEM and TEM images of MY-1 and MY-2 (Figs. 5 and 6, respectively) indicate that the  $\text{Co}_3\text{O}_4$  crystals are formed by aggregation of smaller crystallites during the

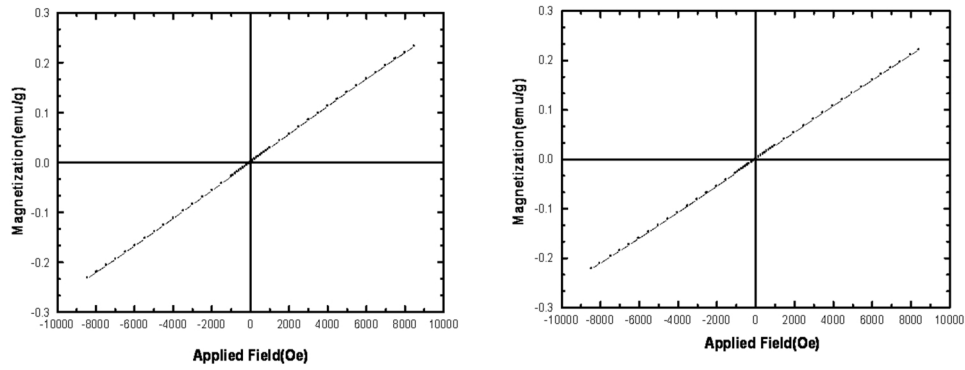


Figure 4.  $(\alpha h\nu)^2$  vs.  $(h\nu)$  of  $\text{Co}_3\text{O}_4$  nanoparticles :MY-1 (left) and MY-2 (right).

synthesis process and the morphology of  $\text{Co}_3\text{O}_4$  nanoparticles is much uniform.

**Conclusion**

Two  $\text{Co}_3\text{O}_4$  nanoparticles, MY-1 and MY-2 with similar morphology are prepared successfully by hydrothermal method using cobalt nitrate and/ acetate in

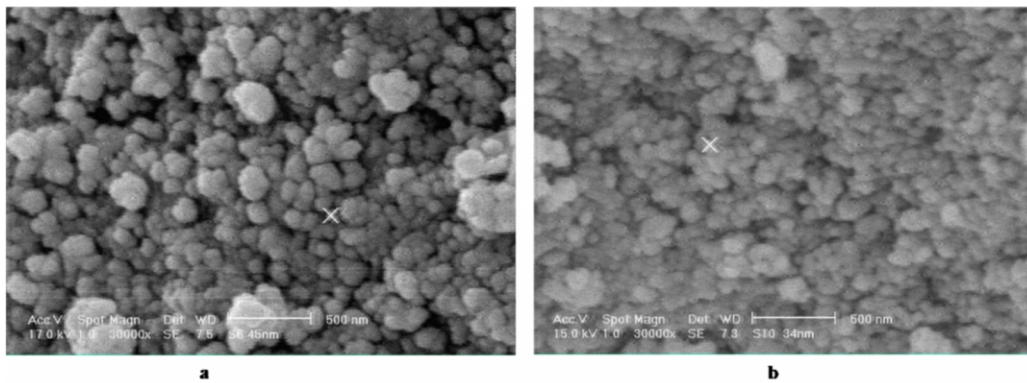


Figure 5. SEM images of  $\text{Co}_3\text{O}_4$  nanoparticles: MY-1 (a) and MY-2 (b).

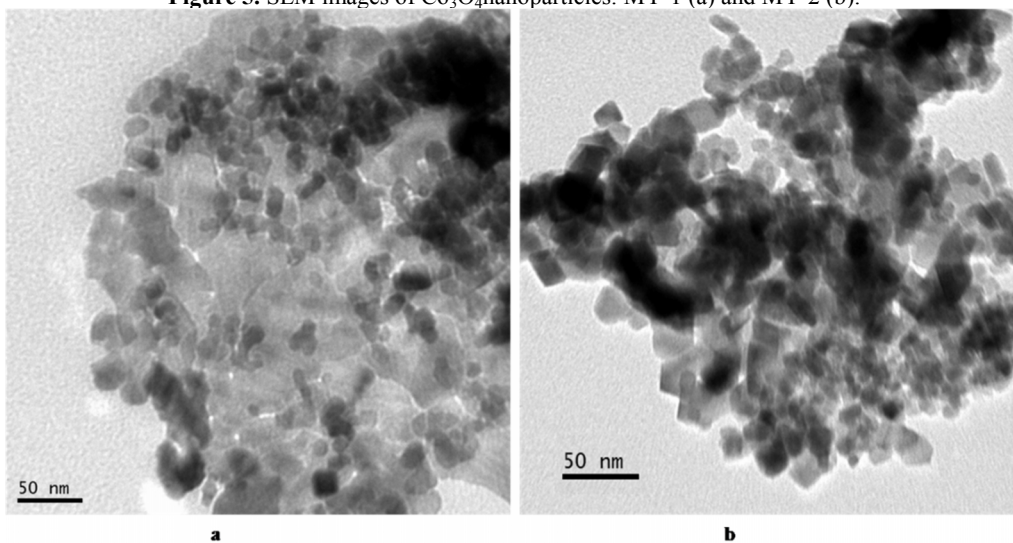


Figure 6. TEM images of  $\text{Co}_3\text{O}_4$  nanoparticles: MY-1 (a) and MY-2 (b).

presence of Triton X-100 as surfactant, and KOH and  $H_2O_2$  as homogeneous precipitating agents. The  $Co_3O_4$  nanoparticles are spherical shaped with an average size 26.6 nm (MY-1) and 21.3 nm (MY-2). They are characterized by FTIR, XRD, SEM and TEM techniques. Optical properties of the  $Co_3O_4$  nanoparticles have revealed the presence of two band gaps 2.9 and 2.4 eV. The vibrating sample magnetometer (VSM) experiments confirm the purity, single phase and paramagnetic behavior.

### References

1. Yuan W. Xie D. Dong Z. Su Q. Zhang J. Du G. and Xu B. Preparation of porous  $Co_3O_4$  polyhedral architectures and its application as anode material in lithium-ion battery. *Mater. Lett.* **97**: 129-132 (2013).
2. Sun C. Su X. Xiao F. Niu C. and Wang J. Synthesis of nearly monodisperse  $Co_3O_4$  nanocubes via a microwave-assisted solvothermal process and their gas sensing properties. *Sens. Actuat. Chem.* **B157**: 681-685 (2011).
3. Manigandan R. Giribabu K. Suresh R. Vijayalakshmi L. Stephen A. and Narayanan V. Cobalt oxide nanoparticles: Characterization and its electrocatalytic activity towards nitrobenzene. *Chem. Sci. Trans.* **2**: S47-S50 (2013).
4. Teng Y. Yamamoto S. Kusano Y. Azuma M. and Shimakawa Y. One-pot hydrothermal synthesis of uniformly cubic  $Co_3O_4$  nanocrystals. *Mater. Lett.* **64**: 239-242 (2010).
5. Lester E. Aksomaityte G. Li, J. Gomez S. Gonzalez-Gonzalez J. and Poliakoff M. Controlled continuous hydrothermal synthesis of cobalt oxide ( $Co_3O_4$ ) nanoparticles. *Prog. Cryst. Growth Charact. Mater.* **58**: 3-13 (2012).
6. Vijayakumar S. Kiruthika Ponnalagi A. Nagamuthu and S. Muralidharan G. Microwave assisted synthesis of  $Co_3O_4$  nanoparticles for high-performance supercapacitors. *Electrochim. Acta.* **106**: 500-505 (2013).
7. Vidal-Abarca C. Lavela P. and Tirado J.L. Cobalt oxide nanoparticles prepared from reverse micelles as high-capacity electrode materials for Li-ion cells. *Electrochim. Solid State Lett.* **11**: A198-A201 (2008).
8. Xu J. Gao L. Cao J. Wang W. and Chen Z. Preparation and electrochemical capacitance of cobalt oxide ( $Co_3O_4$ ) nanotubes as supercapacitor material. *Electrochim. Acta.* **56**: 732-736 (2010).
9. Pan L. Xu M. and Zhang ZD. Synthesis and electrocatalytic properties of  $Co_3O_4$  nanocrystallites with various morphologies. *J. Clus. Sci.* **21**: 655-667 (2010).
10. Hui KS. Hui KN. Yin CL. and Hong X. Synthesis of  $Co_3O_4$  nanowires on nickel foam by a novel microwave-assisted template-free method. *Mater. Lett.* **97**: 154-157 (2013).
11. Ren M. Yuan S. Su L. and Zhou Z. Chrysanthemum-like  $Co_3O_4$  architectures: Hydrothermal synthesis and lithium storage performance. *Solid State Sci.* **14**: 451-455 (2012).
12. Makhlof SA. Bakr ZH. Aly KI. and Moustafa MS. Structural, electrical and optical properties of  $Co_3O_4$  nanoparticles. *Superlat. Microstruct.* **64**: 107-117 (2013).
13. Farhadi S. Pourzare K. and Sadeghinejad S. Simple preparation of ferromagnetic  $Co_3O_4$  nanoparticles by thermal dissociation of the  $[Co^{II}(NH_3)_6](NO_3)_2$  complex at low temperature. *J. Nanostruct. Chem.* **3**: 16-22 (2013).
14. Farhadi S. Pourzare K. and Bazgir S.  $Co_3O_4$  nanoplates: Synthesis, characterization and study of optical and magnetic properties. *J. All. Compd.* **587**: 632-637 (2014).
15. Khalaji AD. Nikookar M. Charles C. Triki S. Thetiot F. and Das D. Facile Preparation of  $Mn_3O_4$  hausmanite nanoplates from a new octahedral manganese (III) Schiff base complex. *J. Clust. Sci.* **25**, 605-615 (2014).
16. Khalaji AD. and Malekan F. Synthesis of  $Mn_3O_4$  nanorods by solid-state thermal decomposition of manganese(III) Schiff base complex  $[Mn(Brsalmeprn)(\mu_{1,3}-N_3)]_n$ . *J. Clust. Sci.* **25**: 517-521 (2014).
17. Hosny NM. Single crystalline  $Co_3O_4$ : Synthesis and optical properties. *Mater. Chem. Phys.* **144**: 247-251 (2014).